CORROSION SCIENCE AND TECHNOLOGY, Vol.31, No.6(2002), pp.468~475

Study on the Naphthenic Acid Erosion-Corrosion Behaviors and Prevention Methods of Carbon Steel

Xinqiang Wu, In Sup Kim, Yugui Zheng*, and Wei Ke*

Nuclear Materials Laboratory, Department of Nuclear Engineering,
Korea Advanced Institute of Science and Technology,
373-1 Kusong-dong, Yusong-gu, Taejon, 305-701, KOREA
**State Key Laboratory for Corrosion and Protection, Institute of Metal Research,*
South District, Chinese Academy of Sciences,
62 Wencui Road, Shenyang 110015, P. R. CHINA

The naphthenic acid erosion-corrosion (NAEC) behaviors of carbon steel, pack-aluminized carbon steel, and carbon steel covered by the high velocity oxygen-fuel (HVOF) thermal sprayed AISI 316L stainless steel coating, were investigated in laboratory and oil refinery. The results revealed that the NAEC rate of carbon steel increases markedly with increase of the velocity of flow, especially in high temperature range. The reasons may be ascribed to the enhanced mass transfer and the accelerated surface reaction as well as the rapid spallation of corrosion products from the metal surface. Both the aluminized carbon steel and the carbon steel covered by the HVOF coating show better resistance against the NAEC relative to the carbon steel due to the higher microhardness and corrosion resistance of their surface-layers. It is recommended the HVOF coating to be applied for NAEC prevention of the components in oil refineries in view of present experimental results.

Keywords *: naphthenic acid, erosion-corrosion, HVOF, pack-aluminized*

1. Introduction

Naphthenic acid erosion-corrosion (NAEC) has been one of the serious problems in the oil-refining installations in spite of many efforts to eliminate or to alleviate this form of attack during last eight decades. Especially in recent years, rapid development of the petroleum industry promotes the exploitation and refining of acidic crude oil increases year-by-year.[1] This results in more aggravating NAEC in oil refineries, especially in the places where the velocity of flow is relatively high such as transfer lines, valves, baffles, furnace tubes, feed and reflux sections of columns, and so on. The accidents caused by the NAEC take place frequently, hampering the safe production and leading to serious economic loss. Since the factors influencing NAEC are very complex and the high-temperature and high-velocity conditions in oil refineries are very difficult to be simulated in laboratory, previous studies on the NAEC primarily depend on the field tests and some low-velocity tests or captive tests in laboratory.[2-4] Since it is unusual to find crude refining units that have run long enough on a single type of crude oil, at relatively constant temperature and acid concentration as well as fixed velocity of flow, the results derived from the field tests may be insufficient to reveal the essence of NAEC and the effect of single factor such as temperature, velocity of flow and acid concentration. Furthermore, it is difficult to reveal the interaction mechanisms between above factors. As for the captive tests in laboratory, due to lack of consideration on the effect of velocity of flow, the test results have little persuasion, too. Therefore, although the petroleum industry has been fighting NAEC for about 80 years, relatively little has been written on this subject during this long time span and most of existing technical papers deal with case histories. At present, material upgrade or surface lining is regarded as the most common and effective way to counteract NAEC in oil refineries except for improving the oil-refining process such as mixture refining, neutralization, adding corrosion inhibitors and so on.[5] Molybdenum-containing stainless steels like AISI 316L and 317L are the primary upgrading or lining materials. However, such upgrade or lining in oil refineries is often eyeless since lack of in-depth understanding on the NAEC and appropriate criterion for material selection, which may cause material waste at some places and NAEC is still very serious at other places.

In view of the circumstances mentioned above, more extensive investigations should be made on NAEC mechanisms of materials used in oil refineries and on improvement of NAEC resistance of these materials. The present paper mainly reports the latest investigations on NAEC behaviors and prevention methods of carbon steel in laboratory and in oil refinery.

2. Experimental

2.1 Experimental samples

The primary test material was hot-rolled carbon steel with the chemical composition (wt.%): 0.16C; 0.20Si; 0.45Mn; 0.30Cu; 0.04P; 0.04S; Fe (balance). The microstructure of carbon steel consisted of ferrite and pearlite and the microhardness was 150. Three kinds of NAEC samples were prepared and investigated in present study. The first was the carbon steel (CS). The second was the pack-aluminized carbon steel (AS). The third was the carbon steel covered by the high velocity oxygen-fuel (HVOF) thermal sprayed AISI 316L stainless steel coating (HS). Since the HS samples were machined from the carbon steel plate with one surface covered by the HVOF coating, only single surface of the HS samples was protected by HVOF coating. Fig. 1 shows the initial surface morphology of the AS samples and the HS samples. X-ray diffraction analysis revealed that the surface-layer of the AS samples was mainly composed of $Fe_{0.5}Al_{0.5}$ phase and the coating of the HS samples was mainly austenite and a little ferrite. The thickness of the aluminized layer of the AS and the coating of the HS was 160 μm and 310 μm respectively. The highest microhardness of surface-layer of two kinds of samples was 530 and 510 respectively. The round samples with diameter of 16 mm were used in laboratory tests and the square samples with size of 70×30 mm were used in field tests.

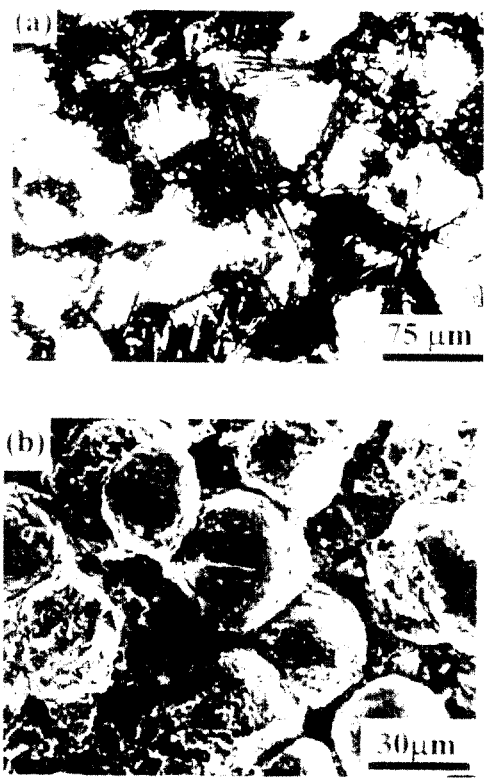

Fig. 1. Surface morphology of (a) AS sample, (b) HS sample

2.2 Experimental installations and mediums

All NAEC experiments were performed by using a set of hot oil loop shown in Fig. 2. A jet impingement equipment combined with a pump was used to realize high velocity of the cyclic medium. The medium in the loop was the mixture of the transformer-oil and the naphthenic acids. The total acid number (TAN) of the cyclic medium in present experiments was 6.0 mgKOH/g.

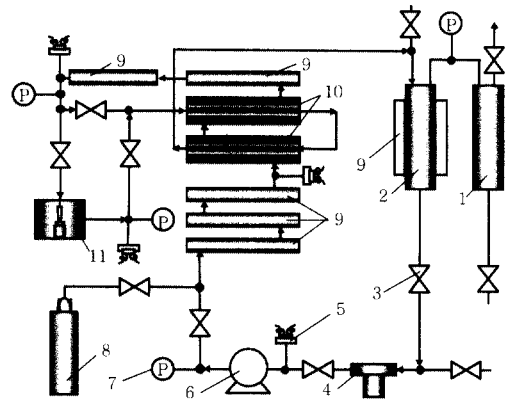

1-releaser, 2-oil reservoir, 3-valve 4-filter, 5- thermocouple, 6-pump, 7-pressure guage, 8-N_2 container, 9-heater, 10-heat exchangers, 11-jet impingement chamber

Fig. 2. Hot oil loop

2.3 Experimental procedures

Before and after NAEC tests, the samples were ultrasonically degreased and rinsed by acetone, dried in air and weighed. The NAEC rate U_{ec} was calculated according to following expression,

$$U_{ec} = \frac{\Delta w_{ec}}{\rho S t} \times 24 \times 365 \quad (1)$$

here ΔW_{ec} is the weight loss only caused by erosion-corrosion, ρ is the density of the test material, S denotes the erosion-corrosion area, and t is the erosion-corrosion

time. During tests, only one surface of samples was normal to the impingement jet, while the other surfaces of samples were soaked in the medium. So the corrosion effect of these surfaces also affected the total weight loss ΔW_t of samples. To diminish this effect, three corrosion samples were soaked parallelly with the erosion-corrosion samples. Then the corrosion rate U_c can be calculated by the weight loss of the parallel corrosion samples. So the weight loss caused by the corrosion for the erosion-corrosion samples, Δw_c, can be obtained. Finally, the weight loss caused only by erosion-corrosion, ΔW_{ec}, can be obtained by subtracting the Δw_c from the ΔW_t.

The field tests were performed in an oil refinery. The test period was 700 days. The test samples were fixed on the support poles of the feeding entry of the atmosphere column, which was one of the most serious erosion-corrosion places in the oil refinery. The test surfaces (the coated surface for the HS samples) were normal to the direction of the jet impingement center of the feeding flow. The field temperature and pressure was 360-365℃ and the normal atmosphere, respectively. The medium was the bottom oil of primary distillation tower with TAN of 0.9-1.2 mgKOH/g and sulfur content of 0.8-1.0%.

A JSM-6301F scanning electron microscopy was used for NAEC morphology observation.

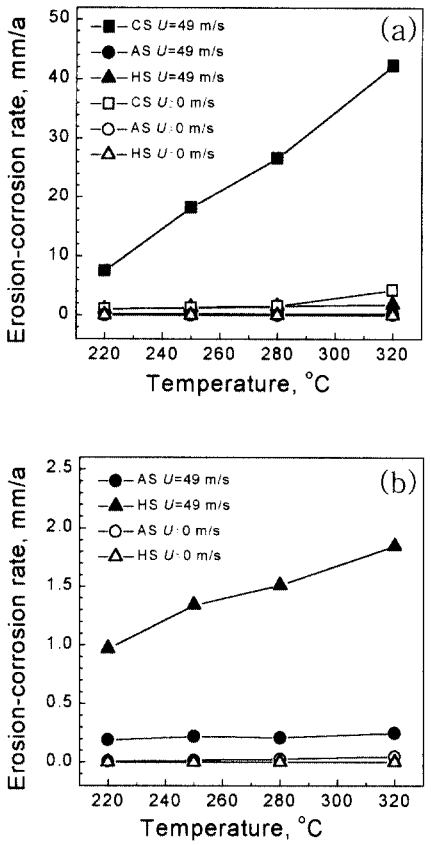

Fig. 3. NAEC rate at high temperature of (a) CS, AS and HS, (b) AS and HS

3. Results and discussion

3.1. Laboratory tests results

Fig. 3 shows the NAEC rate of the CS, AS and HS. Obviously, the NAEC rate increased with increase of the velocity of flow, especially for the CS (Fig. 3a). Increasing temperature markedly accelerated the NAEC of the CS. For example, at 320℃, the NAEC rate under the fast flow (the velocity of flow is 49 m/s) was almost 10 times as that under the slow flow (the velocity of flow is ≅ 0 m/s). However, the AS and HS showed much better NAEC resistance compared to the CS (Fig. 3a). The detailed NAEC rate in Fig. 3b revealed that under the fast flow the AS had better resistance against the NAEC than the HS. Moreover, the difference between the AS and HS tended to increase with temperature.

Fig. 4 shows the surface morphology of the CS samples after 10 h NAEC. With increase of the velocity of flow or the temperature, the NAEC of the CS was aggravated markedly. At 250℃ and under the slow flow, some residual metal scraps appeared along the grain boundaries and were connected with the corrosion pits or cracks (shown by arrowheads in Fig. 4a). Under the fast flow, many parallel and continuous erosion-corrosion grooves were produced on the sample surface. Two different zones, A and B, were formed (Fig. 4b). The grooves in zone A were deeper than those in zone B, from which zone B was raised relative to zone A. The grooves at the boundaries of zone A and zone B were continuous. There also existed some metal scraps of smaller size. After 10 h erosion-corrosion at 280℃, the grooves with wider space appeared. However, the grooves only kept the same orientation in local area rather than in most of area. The erosion-corrosion ridges between the grooves were not continuous as those at 250℃ and were similar to the fragmentary wall (Fig. 4c). After 10 h erosion-corrosion at 320℃, some areas became relatively smooth and some areas kept still rough. A smoother transition zone (C) appeared between the two kinds of areas (Fig. 4d).

After 10 h erosion-corrosion under the slow flow at 250℃, the surface of the AS samples was damaged slightly. Only some small cracks and pits appeared at grain boundaries (Fig. 5a). When the velocity of flow was increased to 49 m/s, the cracks and the pits along the grain boundaries became more marked (Fig. 5b). After 10 h erosion-corrosion under the fast flow at 280℃, the cankerous morphology appeared near grain boundaries (Fig. 5c). After erosion-corrosion at 320℃, the cankerous morp-

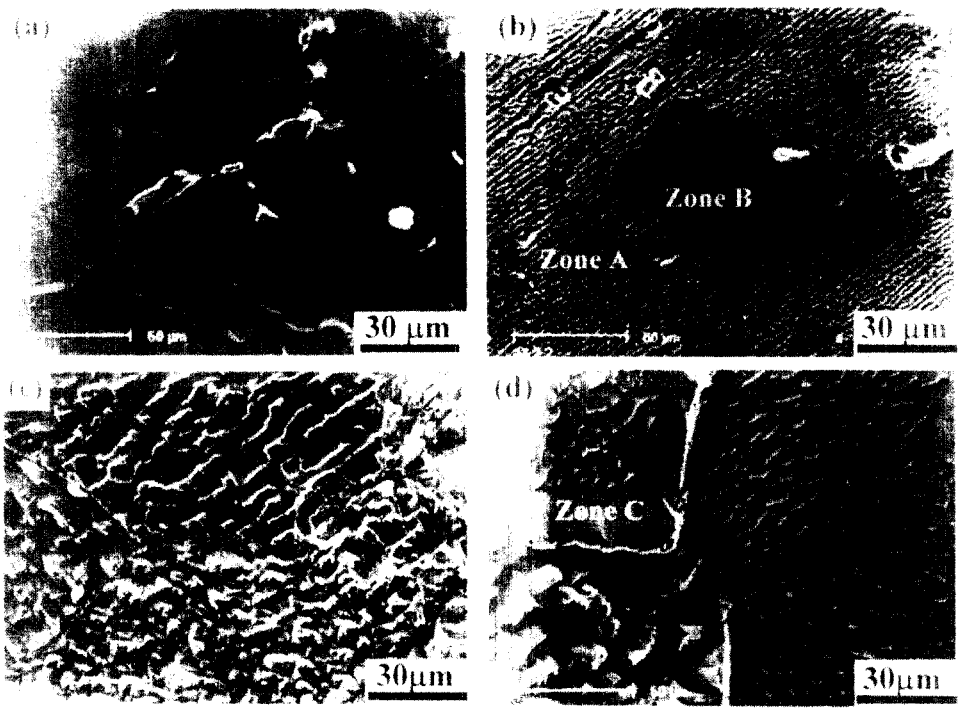

Fig. 4. NAEC morphology of CS (TAN=6.0 mgKOH/g, t=10 h) (a) 250℃, ≅0 m/s (b) 250℃, 49 m/s (c) 280℃, 49 m/s (d) 320, 49 m/s

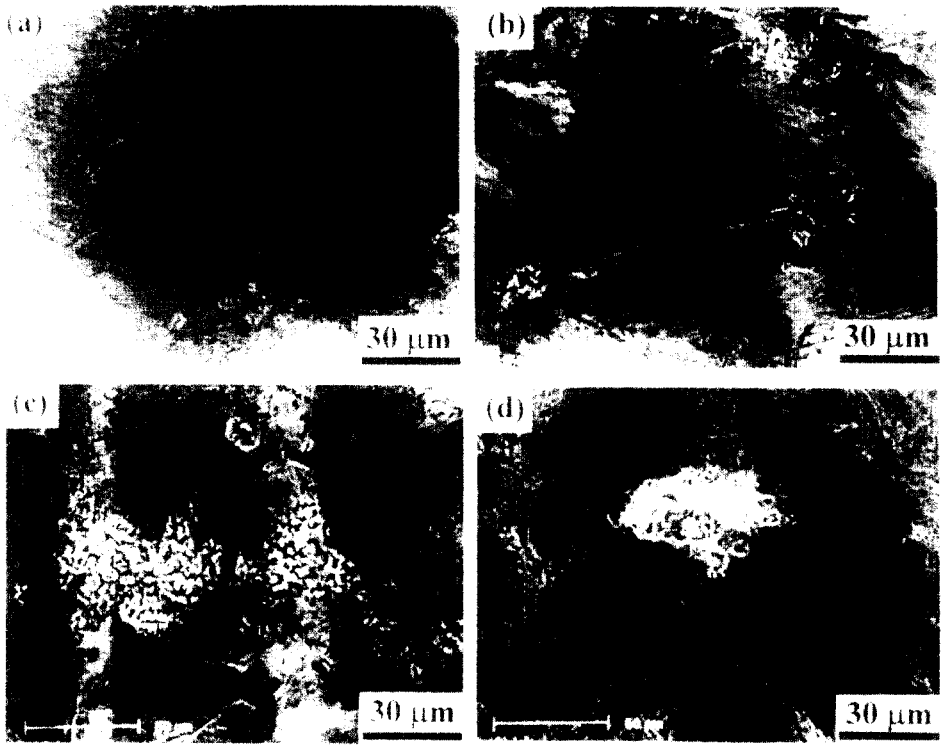

Fig. 5. NAEC morphology of AS (TAN=6.0 mgKOH/g, t=10h) (a) 250℃, ≅0 m/s (b) 250℃, 49 m/s (c) 280℃, 49 m/s (d) 320℃, 49 m/s

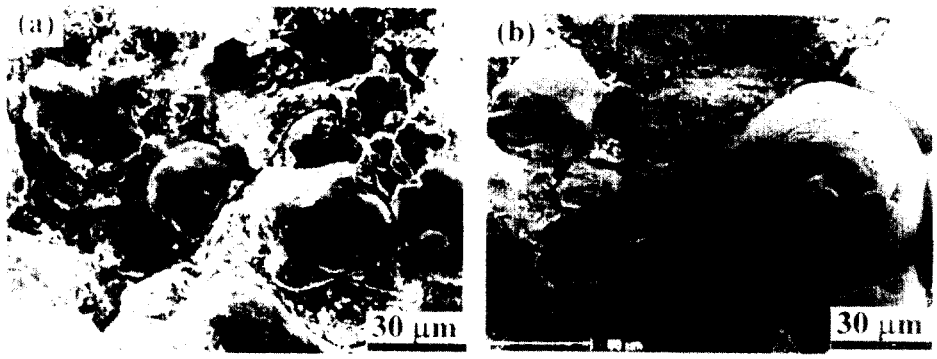

Fig. 6. NAEC morphology of HS (TAN=6.0 m/s, t=10 h) (a) 250℃, 49 m/s (b) 320℃, 49 m/s

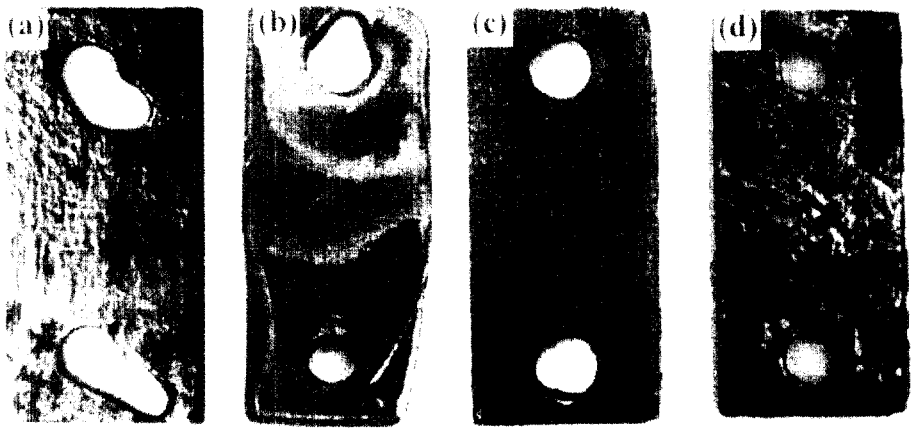

Fig. 7. Macromorphology of the samples after 700-days field test (a) CS (b) AS (c) the coated surface of HS (d) the uncoated surface of HS

hology became more frequent and the spallation took place at local areas (Fig. 5d). For HS, at lower temperature and under the slow flow, the coated surface had little change after erosion-corrosion. This was consistent with the very low erosion-corrosion rate of HS shown in Fig. 3b. With increase of the temperature and the velocity of flow, slight damage took place on the coated surface of HS (Fig. 6a). At 320℃, the damage caused by erosion-corrosion was aggravated. Some metal particles had cracked and their skin had been damaged distinctly (Fig. 6b).

3.2 Field test results

The results of field tests are listed in Table 1. In practical oil-refining environment, the CS showed little resistance against the erosion-corrosion relative to the AS and HS, too. The erosion-corrosion rate of the HS was slightly higher than that of the AS. However, the thickness change of the HS samples was about half of that of the AS samples. Moreover, it can be clearly seen from the surface morphology in Fig. 7 and Fig. 8 that the coated surface of the HS showed the best resistance against the erosion-corrosion during the field tests. After 700-days test, the coating of the HS still kept integral (Fig. 7c), only slight erosion-corrosion traces appeared on the surface of metal particles of the coating (Fig. 8c and Fig. 8d). But the surfaces of the CS and the AS had been damaged seriously and the samples had been deformed (Fig. 7a, Fig. 7b and Fig. 8a, Fig. 8b). It should be noted that the erosion-corrosion of another surface of the HS was also serious as shown in Fig. 7d since this surface was the bare carbon steel without the HVOF coating. However, the erosion-corrosion rate of the HS in Table 1 was calculated by

Table 1. Erosion-corrosion and thinning rate of samples tested in oil refinery

Sample code	CS	AS		HS	
	CS-1	AS-1	AS-2	HS-1	HS-2
Erosion-corrosion rate, mm/a	0.384	0.116	0.088	0.116*	0.129*
Thinning rate**, mm/a	0.976	0.136	0.115	0.068	0.073

* : erosion-corrosion rate on the assumption that all surfaces of HS samples were covered by HVOF coating.

** : thinning rate=365((the initial thickness-the thickness after test)/700.

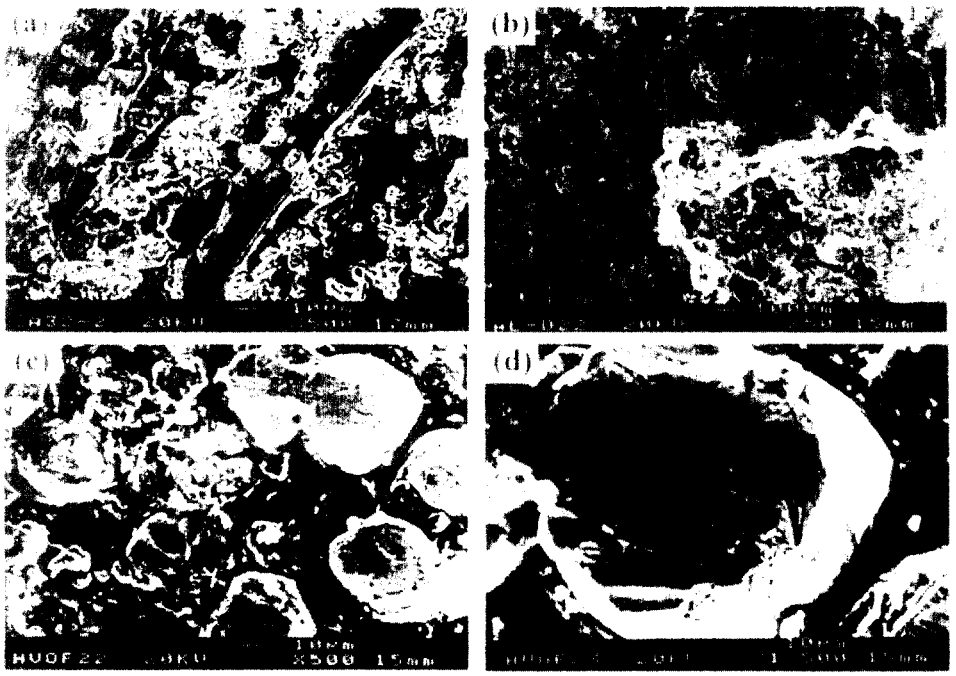

Fig. 8. High magnification morphology of the samples after 700-days field test (a) CS (b) AS (c) HS (d) the high magnification of (c)

assuming that all the surfaces of the HS samples were covered by the HVOF coating. Since the calculated erosion-corrosion rate did not include the influence of the bare carbon steel surfaces of the HS samples, they were higher than the real erosion-corrosion rate of the HVOF coating.

3.3 Discussion

The naphthenic acid corrosion (NAC) can be regarded as pure chemical corrosion since the naphthenic acid medium is non-electrolyte. The usual corrosion mechanism is as follows:

$$2nRCOOH + 2M \rightarrow 2M(RCOO)_n + nH_2 \quad (2)$$

here R denotes the naphthenic radical, M denotes the active metal (Fe), and $M(RCOO)_n$ denotes the corrosion product and can dissolve in the naphthenic acids or oil mediums. The NAC process usually includes: the transportation of the naphthenic acid molecules toward the metal surface, the surface absorption of the naphthenic acid molecules, the active reactions on metal surface, and the spallation of corrosion products from the metal surface, each of which may influence the total corrosion process. There are different point of views on the control-step of NAC. Gutzeit *et al.* found the NAC kinetics obeys the Arrnius equation when the temperature was beyond the 280℃.[6] The calculated activation energy was 68.5 kJ/mol. They concluded that the control-step of NAC was the surface chemical absorption. Based on the results of Gao *et al.*, the NAC kinetics of carbon steel coincided with the Arrinus rule in the temperature range of 150-210℃.[7] The calculated activation energy was 346 kJ/mol. They suggested the control-step of NAC was the active surface reaction. According to the activation energy, the naphthenic acid corrosion is an endothermic reaction, so increasing temperature accelerates the active reaction. However, based on the absorption theory, both physical absorption and chemical absorption are spontaneous process, the process free energy decreases when the absorption takes place, *i.e.*, $\Delta G<0$. When the naphthenic acid molecules are absorbed on the metal surface, their motion is limited to surface motion from the free motion in the liquid. The free degree of motion is decreased. So the entropy is decreased, i.e., $\Delta S<0$. In terms of the thermodynamic equation,

$$\Delta G = \Delta H - T\Delta S \quad (3)$$

$\Delta H<0$. So the absorption of naphthenic acid molecules on metal surface is an exothermic process. Increasing the temperature will retard the absorption of naphthenic acid molecules. Therefore, the control-step of NAC is closely related to the corrosion temperature. At higher tem-

perature, the active reaction on metal surface is easy, the surface absorption is relatively difficult, so the surface absorption may become the control-step of NAC as suggested by Gutzeit *et al.* At lower temperature, although the surface absorption becomes relatively easy, there is lack of the active molecules, the surface reaction is retarded, so the active reaction may become the control-step of NAC as suggested by Gao *et al.* The test temperature in present work is in the middle range, so it is difficult to determine which one is the primary control-step of NAC.

Increasing the velocity of flow, the NAEC rate increased rapidly (Fig. 3a). The corresponding NAEC morphology also revealed that the surface damage was observably aggravated (Fig. 4 and Fig. 5). The hydromechanical parameters usually affect the erosion-corrosion behaviors by changing the erosion strength or the mass transfer process. For static mediums, the transfer of the naphthenic acid molecules towards the metal surface mainly relies on the diffusion. But for flowing mediums, the total transfer process of the naphthenic acid molecules includes the convection and the diffusion. In this case, the mass transfer rate can be expressed by the dimensionless Sherwood number,

$$\mathrm{Sh} = KL / D_i \tag{4}$$

here K is the mass transfer coefficient, L is the characteristic size, and D_i is the diffusion coefficient. For the jet impingement flow in present tests, Sh can be rewritten as follows[8]:

$$\begin{aligned} &\mathrm{Sh} = \alpha\, \mathrm{Re}^{x}\, \mathrm{Sc}^{y} f(H/d) f(r/d) \\ &\mathrm{Re} = Ud / \gamma \\ &\mathrm{Sc} = \gamma / D_i \end{aligned} \tag{5}$$

here Re is the Reynold's number, Sc is the Smitt number. *f(H/d)* and *f(r/d)* are the geometry factors. U is the exit velocity of the nozzle, γ is the kinetic viscosity. Obviously, the transfer rate increases with increase of the velocity of flow. Moreover, the grooves formed on the metal surface under the fast flow give rise to the increase of surface roughness and specific surface (Fig. 4). Based on the results of Kappesser et al. and Gabe *et al.*,[9-10] the increasing roughness induces the increase of the mass transfer rate; the increasing specific surface may induce the surface micro-turbulence and thus accelerate the mass transfer. So the fast flow promotes the transfer of the naphthenic acid molecules towards the metal surface, and in turn enhances the NAC. In addition, in terms of the wall shear stress of jet impingement flow,[1]

$$\tau = 0.0112 \rho U^2\, \mathrm{Re}^{-0.182} [r / r_0]^{-2.0} \tag{6}$$

the τ is proportional to U. So increasing the velocity of flow may enhance the erosion strength. Moreover, the wall shear stress contributes an added mechanical means to remove the corrosion product films from the metal surface. Thus increasing the velocity of flow accelerates the spallation of corrosion product and induces more fresh metal surface contact directly with the naphthenic acid mediums. As a result, the NAEC is aggravated.

The different NAEC morphology in different zones on the CS surface may be associated with the initial surface situation of samples. Since the CS samples were machined from the hot-rolling plate, there may exist some difference in the hot-rolling surface-layer such as the orientation, the deformation degree, and the stored energy among different crystals. Such heterogeneity may result in difference of corrosion resistance and hardness among different crystals. During NAEC, some crystals in corrosion-susceptible orientation or with lower hardness may be corroded or eroded firstly, which results in the heterogeneous NAEC morphology (Fig. 4).

Both laboratory and field tests showed that the AS and HS had much better resistance against the NAEC than the CS. This may be ascribed to the higher microhardness and the better corrosion resistance of surface-layer of the AS and HS. As stated previously, the microhardness of surface-layers of the AS and HS is about three or four times than that of the CS. Such high microhardness contributes a good resistance to the erosion of flow. In addition, the aluminized layer of the AS can effectively prevent the direct contact between the corrosion mediums and the carbon steel matrix. The HVOF coating of the HS is rich in corrosion-resistant elements such as Cr, the most primary element to form protective oxide film on the coated surface, and Mo, the most effective element to resist the NAC.[11] So, both AS and HS inhere in good resistance against the NAEC.

It should be noted that there is a contradiction between the NAEC rate and the NAEC morphology for the HS. The NAEC rate (Fig. 3b and Table 1) of the HS was slightly higher than that of the AS. But the NAEC morphology (Fig. 5 to Fig. 8) revealed that the HVOF coating of the HS was more effective to protect the matrix than the aluminized layer of the AS, especially in the field tests. It is believed that such a contradiction mainly results from the preparation of the HS samples because only single surface of the HS samples was covered by the HVOF coating. For laboratory tests, although the weight loss caused by the corrosion of carbon steel surfaces had

been considered in the calculation of NAEC rate, the weight loss due to the corrosion of the interface between the coating and matrix was difficult to be estimated and have to be neglected. Thus the calculated NAEC rate was larger than the real NAEC rate of the HVOF coating. For field tests, since different surfaces of the HS samples were subject to different erosion-corrosion strength, it was difficult to estimate the weight loss due to the erosion-corrosion of the carbon steel surfaces. The erosion-corrosion rate was calculated on the assumption that all surfaces were covered by the HVOF coating. This resulted in underestimation of the real resistance of the HVOF coating against the erosion-corrosion since the carbon steel surfaces of the HS samples were seriously eroded during the tests (Fig. 6d). However, in spite of above problems, it can be seen clearly by the erosion-corrosion morphology that the HVOF coating investigated currently showed the excellent resistance against the NAEC. In addition, the HVOF coating inheres in some other attractive characteristics such as very rapid spraying velocity and controllable thermal influence on the matrix, which will prevent the matrix from deformation, thermal-stress and metallurgical change during spraying operation.[12] So, if improved work is developed, it is believed that the HVOF coating may be applied for future NAEC prevention of the components in oil refineries.

4. Conclusions

1) The control-step of NAC is closely related to the corrosion temperature.

2) The N EC rate of carbon steel increases markedly with increase of the velocity of flow, especially in high temperature range. The reasons may be ascribed to the enhanced mass transfer and the accelerated surface reaction as well as the rapid spallation of corrosion products from the metal surface.

3) The aluminized carbon steel and the carbon steel covered by the HVOF coating show better resistance against the NAEC relative to the carbon steel in both laboratory tests and field tests due to the higher microhardness and corrosion resistance of their surface-layers.

4) Despite the HVOF coating needs improvement, it is recommended the coating to be applied for NAEC prevention of the components in oil refineries in view of present experimental results.

Acknowledgements

The financial supports received partially from the Brain Korea 21 and the Innovation Fund of IMR of CAS are gratefully acknowledged.

References

1. R. D. Kane and M. S. Cayard, *Mater. Perform.*, **38**, 48 (1999).
2. M. J. Zetlmeisl, in *Corrosion'96*, 218 (1996).
3. A. Turnbull, E. Slavcheva and B. Shone, *Corrosion*, **54**, 922 (1998).
4. E. Slavcheva, B. Shone, and A. Turnbull, *Brit. Corros. J.*, **34**, 125 (1999).
5. A. Jayaraman and R. C. Saxena, *Corros. Prevent. Contr.*, **42**, 123 (1995).
6. J. Gutzeit, *Mater. Perform.*, **16**, 24 (1977).
7. Y. M. Gao, J. J. Cheng, G. Yu, H. Y. Yang, D. Z. Cao, and Y. J. Zhu, *Corros. Sci. Protect. Technol. (in Chinese)*, **12**, 27 (2000).
8. B. Poulson, *Corros. Sci.*, **23**, 391 (1983).
9. R. Kappesser, I. Cornet, and R. Grife, *J. Electrochem. Soc.*, **118**, 1957 (1971).
10. D. R. Gabe and P. A. Makanjuola, *J. Appl. Electrochem.*, **17**, 370 (1987).
11. H. L. Jr. Craig, in *Corrosion'96*, 603 (1996).
12. L. N. Moskowitz, *J. Therm. Spray Technol.*, **2**, 21 (1993).